ARTICLE
Journal of Cellular Biochemistry 107:933–943 (2009)

Journal of Cellular Biochemistry

Reactive Oxygen Species-Induced Cell Death of Rat Primary Astrocytes Through Mitochondria-Mediated Mechanism

Chia-Chun Wang,[1] Kuan-Min Fang,[1] Chung-Shi Yang,[2,3]* and Shun-Fen Tzeng[1]**

[1]*Department of Life Sciences, National Cheng Kung University, Tainan City, Taiwan*

[2]*Department of Applied Chemistry, Graduate Institute of Biomedicine and Biomedical Technology, National Chi-Nan University, Puli, Taiwan*

[3]*Center for Nanomedicine Research, National Health Research Institutes, Zhunan, Taiwan*

ABSTRACT

Astrocytes, the most abundant glial cell population in the central nervous system (CNS), play physiological roles in neuronal activities. Oxidative insult induced by the injury to the CNS causes neural cell death through extrinsic and intrinsic pathways. This study reports that reactive oxygen species (ROS) generated by exposure to the strong oxidizing agent, hexavalent chromium (Cr(VI)) as a chemical-induced oxidative stress model, caused astrocytes to undergo an apoptosis-like cell death through a caspase-3-independent mechanism. Although activating protein-1 (AP-1) and NF-κB were activated in Cr(VI)-primed astrocytes, the inhibition of their activity failed to increase astrocytic cell survival. The results further indicated that the reduction in mitochondrial membrane potential (MMP) was accompanied by an increase in the levels of ROS in Cr(VI)-primed astrocytes. Moreover, pretreatment of astrocytes with *N*-acetylcysteine (NAC), the potent ROS scavenger, attenuated ROS production and MMP loss in Cr(VI)-primed astrocytes, and significantly increased the survival of astrocytes, implying that the elevated ROS disrupted the mitochondrial function to result in the reduction of astrocytic cell viability. In addition, the nuclear expression of apoptosis-inducing factor (AIF) and endonuclease G (EndoG) was observed in Cr(VI)-primed astrocytes. Taken together, evidence shows that astrocytic cell death occurs by ROS-induced oxidative insult through a caspase-3-independent apoptotic mechanism involving the loss of MMP and an increase in the nuclear levels of mitochondrial pro-apoptosis proteins (AIF/EndoG). This mitochondria-mediated but caspase-3-independent apoptotic pathway may be involved in oxidative stress-induced astrocytic cell death in the injured CNS. J. Cell. Biochem. 107: 933–943, 2009.

KEY WORDS: GLIA; OXIDATIVE STRESS; APOPTOSIS INDUCING FACTORS; CASPASE-3; *N*-ACETYLCYSTEINE; MITOCHONDRIA

Astrocytes, the major glial cell population in the central nervous system (CNS), provide the structural and metabolic support to neurons and regulate the neuronal synaptic transmission [Chen and Swanson, 2003]. These cells also serve to maintain the homeostasis of pH, ions, and neurotransmitters in the synaptic space [Koehler et al., 2006]. In terms of their structure, these cells have extended processes called footplates or end-feet, which surround the vascular surfaces of the brain and pia tissues to form perivascular–glial and pial–glial limiting membranes [Voutsinos-Porche et al., 2003; Koehler et al., 2006]. Their cell bodies are juxtaposed between neurons and the capillary endothelium to form the blood–brain barrier (BBB). Thus, given these cytoarchitectural features, astrocytes are the first cells of the brain parenchyma to encounter foreign molecules that cross the BBB [Tiffany-Castiglioni et al., 1989], pointing to the importance of astrocytes in the maintenance of BBB integrity. In addition, astrocytes have the critical role of scavenging free radicals since these cells are the source of antioxidants (such as GSH) and antioxidative enzymes (i.e., superoxide dismutase, SOD; glutathione peroxidase, GPx). Accordingly, astrocytes are believed to provide physical and chemical protection of CNS neurons against oxidative stress [Kraig et al., 1995; Ransom et al., 2003; Li et al., 2008].

Additional Supporting Information may be found in the online version of this article.

Grant sponsor: National Science Council, Taiwan; Grant numbers: NSC 96-2321-B-006-006-MY3, NSC 96-2120-M-260-001.

*Correspondence to: Chung-Shi Yang, Department of Applied Chemistry, Graduate Institute of Biomedicine and Biomedical Technology, National Chi-Nan University, Puli, Taiwan. E-mail: cyang@nhri.org.tw

**Correspondence to: Shun-Fen Tzeng, Department of Life Sciences, National Cheng Kung University, #1 Ta-Hsueh Road, Tainan City 70101, Taiwan. E-mail: stzeng@mail.ncku.edu.tw

Received 29 December 2008; Accepted 3 April 2009 • DOI 10.1002/jcb.22196 • © 2009 Wiley-Liss, Inc.

Published online 20 May 2009 in Wiley InterScience (www.interscience.wiley.com).

Chromium (Cr), a redox-active transition metal, is considered as a potent carcinogen by the International Agency for Research on Cancer (IARC). Cr(VI) is a powerful oxidant, and can interact with cellular reductants to generate intermediate oxidation state, such as Cr(V) and Cr(IV), as well as Cr(III) which is the final oxidation state [Bagchi et al., 2002; Harris and Shi, 2003]. While Cr(VI) is converted to Cr(V)–Cr (III), reactive oxygen species (ROS), such as superoxide anion, hydrogen peroxide singlet oxygen, and hydroxyl radicals, are produced which induce oxidative stress, DNA damage and altered gene expression, as well as cell apoptosis [Shi and Dalal, 1994; Kasprzak, 2002; O'Brien et al., 2003; Costa and Klein, 2006]. Cr(VI)-induced ROS generation is also considered as the critical players of Cr(VI) carcinogenicity and toxicity due to the induction of DNA lesions, such as Cr–DNA adduct, DNA strand breaks, and DNA–DNA crosslinks [Sugiyama et al., 1986; Chen et al., 2001; Ding and Shi, 2002; Harris and Shi, 2003; O'Brien et al., 2003].

Oxidative injury is associated with the neuropathogenesis of acute and chronic CNS neurodegenerative disorders [Love, 1999; Andersen, 2004]. Since astrocytes have critical neuroprotective functions in the CNS, it is important to understand how astrocytes respond to oxidative insults. Our previous study has reported that exposure to the redox-inactive metal, cadmium, induced the disruption of intracellular Ca^{2+} homeostasis by robust Ca^{2+} influx and increased intracellular ROS in astrocytes, which triggered a Ca^{2+}/ROS-dependent but caspase-3 independent pathway to result in astrocytic cell death [Yang et al., 2008]. In the present study, we used the redox active metal, Cr(VI), as a chemical oxidant which did not induce Ca^{2+} influx into astrocytes, but can significantly increase ROS production in astrocytes. Herein, we provide evidence that ROS generated in Cr(VI)-primed rat cortical astrocytes induced the decline in mitochondrial membrane potential (MMP), which subsequently could result in nuclear translocation of mitochondrial pro-apoptosis proteins (apoptosis-inducing factor, AIF; endonuclease G, EndoG), leading to astrocytic apoptosis through a mitochondria-mediated and caspase-3-independent mechanism.

MATERIALS AND METHODS

MATERIALS

Media and antibiotics were purchased from Invitrogen (Carlsbad, CA). Cell cultureware and Petri dishes were obtained from BD Biosciences (San Jose, CA). Fetal bovine serum (FBS) and calf serum (CS) were the products of Hyclone Laboratories (Logan, UT). Poly-D-lysine (PDL), *N*-acetylcysteine (NAC), MTT, protease inhibitor cocktail, potassium chromate (K_2CrO_4), and other chemicals were purchased from Sigma–Aldrich (St. Louis, MO). Lactate dehydrogenase (LDH) assay kit and caspase-3 activity assay kit were from Roche Diagnostics (Indianapolis, IN) and Promega (Madison, WI), respectively. Caspase-3 colorimetric assay kit was from R&D System (Minneapolis, MN). T4 polynucleotide kinase and nuclear factor κB (NF-κB)/activating protein-1 (AP-1) consensus sequences were purchased from Promega. The specific inhibitor for caspase-3, Z-DEVD-FMK, was purchased from Tocris Bioscience (Ellisville, MI). NE-PER® nuclear extraction reagent and 4′, 6-diamidine-2′-phenylindole, dihydrochloride (DAPI) were from Pierce (Rockford, IL). Antibodies used in this study were listed as follows: rabbit anti-AIF antibody, IgG (Santa Cruz Biotechnology, Santa Cruz, CA; Cell Signaling Technology, Danvers, MA), rabbit anti-EndoG (Chemicon, Temecula, CA; Cell Signaling Technology), rabbit anti-caspase-3 antibody (Cell Signaling Technology), anti-histone 1 (H1) antibody (Santa Cruz Biotechnology), horseradish peroxidase (HRP)-conjugated secondary antibody (Jackson ImmunoResearch Laboratories, West Grove, PA), biotinylated secondary antibodies, and fluorescein–avidin D (Vector Laboratories, Burlingame, CA). Apo-BrdU TUNEL assay kit was the products from Invitrogen/Molecular Probes (Eugene, OR). Immobilon nitrocellulose (NC) membrane and enhanced chemiluminescence (ECL) solution were the products of Millipore (Bedford, MA) and Perkin Elmer (Boston, MA), respectively. Glutathione assay kit was from Cayman (Ann Arbor, MI).

PRIMARY CULTURE

Primary neuronal and mixed glial cultures were prepared as previously described [Yang et al., 2008]. In brief, cerebral cortices were removed from embryonic days 17–18 or 1–2-day-old Sprague–Dawley rat brains for neuronal and mixed glial cultures, respectively. The tissue was dissociated in 0.0025% trypsin/EDTA and passed through a 70-μm pore nylon mesh. After centrifugation, the cell pellet was resuspended in DMEM/F-12 containing 10% FBS, 50 U/ml penicillin, and 50 mg/ml streptomycin. Neuronal cells were seeded at the density of 1×10^5 cells/well onto a 24-well plates coated with 0.0025% PDL in 0.1 M boric acid buffer, and cultured in DMEM/F-12 containing 10% heat-inactivated horse serum for 2 h at 37°C, 5% CO_2. The medium was then changed with Neurobasal medium containing 1× B-27 serum supplement for every 2 days, and the cultures were maintained in Neurobasal medium plus B-27 for 9–10 days. Alternatively, mixed glial cells (10^7 cells/flask) were then plated onto PDL-coated T75 tissue culture flasks. The medium was renewed every 2–3 days. Eight days later, microglia were removed by shaking [McCarthy and de Vellis, 1980]. Astrocytes were replated either onto 35, 60, or 100 mm tissue culture dishes at a density of 4×10^5, 1×10^6, or 5×10^6 cells/dish, respectively. Three days later, the cells were treated with K_2CrO_4 at different concentrations in DMEM medium for distinct time periods. In general, the cultures consisted of 90–92% astrocytes (as indicated by GFAP-positive staining), whereas less than 10% of cells were microglia and oligodendrocytes.

CELL VIABILITY ASSAY

To study the effect of K_2CrO_4 on the cell viability of astrocytes, cells were treated with K_2CrO_4 in serum-free DMEM medium for distinct time periods, followed by the MTT assay. The assay was performed as previously described [Yang et al., 2008]. In brief, MTT solution (5 mg/ml) was added to each well for 4 h. The culture then was incubated with SDS (10% in 0.01 N HCl) overnight at 37°C. MTT absorbance was measured using an ELISA reader at 595 nm. The data are presented as the percentage versus control which represents 100% cell viability.

LDH ASSAY

Cell cytotoxicity analysis by measuring the LDH activity in the culture medium was performed to validate MTT cell viability. The

cultured supernatant was collected, centrifuged at 1,500 rpm for 10 min to remove cell debris, and subsequently processed for the LDH assay following the procedure provided by the vendor. The data are presented as the relative LDH activity (a fold of control).

WESTERN BLOTTING

After treatment, the cells were harvested and gently homogenized on ice using phosphate-buffered saline (PBS) containing SDS, 1 mM phenylmethylsulfonyl fluoride (PMSF), 1 mM EDTA, 1 mM sodium orthovanadate, and proteinase inhibitor cocktail. Nuclear proteins were extracted from astrocytes (5×10^6 cells/100-mm dish) treated with K_2CrO_4 for 6 h by using NE-PER® nuclear extraction reagents (Pierce), following the procedure provided by the vendor. The lysate was centrifuged at 10,000 rpm for 10 min. Protein concentration was determined by using a Bio-Rad DC kit (Hercules, CA). Total proteins (30–50 μg) or nuclear proteins (30 μg) were separated by 10% SDS–PAGE and transferred to NC membrane. The membrane was then probed with anti-AIF, anti-EndoG, or anti-H1 antibodies overnight at 4°C, and then incubated with HRP-conjugated secondary antibodies for 1 h at room temperature. The detection was carried out by using ECL solution.

DNA FRAGMENTATION ANALYSIS

Astrocytes (5×10^6 cells/100-mm dish) were treated with K_2CrO_4 for 6 and 12 h. After harvesting, the cells were incubated in 500 μL lysis buffer (20 mM Tris–HCl, pH 7.5, 10 mM EDTA, and 0.2% Triton X-100) on ice for 10 min, and then centrifuged at 12,000 rpm for 10 min. The supernatant was treated with proteinase K (200 μg/ml) at 50°C for 8 h, followed by the addition of RNase A (100 μg/ml) at 37°C for 6 h. DNA was extracted by phenol–chloroform–isoamyl alcohol (25:24:1) and isopropanol precipitation. Samples were electrophored on a 2% agarose gel at 70 V for 1 h, stained with ethidium bromide, and then photographed under UV illumination. Bio-100 bp DNA ladder was used as a DNA size marker.

TUNEL APOPTOSIS ASSAY

Astrocytes were replated onto 100 mm Petri dishes at 2×10^6 cells per dish, and 2–3 later treated with K_2CrO_4 for 12 h. DNA fragmentation that is the characteristic of cellular apoptotic cells can generate large amounts of 3′-hydroxyl DNA ends which can be labeled by adding the deoxythymidine analog BrdU using the method of terminal deoxynucleotide transferase dUTP nick end labeling (TUNEL). In brief, the cells were trypsinized using trypsin–EDTA, and fixed with 1% paraformaldehyde in cold PBS for 15 min. Cells were incubated in ice-cold 70% ethanol at −20°C overnight, and then followed by using Apo-BrdU TUNEL assay kit under the instructions provided by the vendor. The samples were processed by flow cytometry (BD FACSCalibur) to quantify apoptotic cells.

CASPASE-3 ACTIVITY ASSAY

The assay was followed by the procedure as previously described [Yang et al., 2008]. Briefly, astrocytes (5×10^6 cells/100-mm dish) were treated with K_2CrO_4 in DMEM for 12 and 24 h. These cells were collected and lysed in the lysis buffer provided by the vendor. Total protein in cell lysate was measured by using a Bio-Rad DC kit. The cell lysate (50 μg) was incubated with a caspase-3 substrate Ac-DEVD-pNA for 2 h, and then processed for the colorimetric assay of caspase-3 activity. The caspase-3 activity was measured by monitoring the intensity of free pNA (yellow color) by an ELISA reader at 405 nm. The data are presented as the percentage versus control (100% activity).

CELLULAR ROS MEASUREMENT

ROS production was analyzed with CM-H_2 DCFDA [Li et al., 2005], which is converted by endogenous esterases to carboxy-H_2 DCF and then oxidized to the fluorescent probe (CM-DCF) after exposure to ROS. Primary astrocytes were preincubated with 10 μM CM-H_2 DCFDA at 37°C for 45 min, followed by treatment with desired concentrations of K_2CrO_4 for 6, 12, and 15 h. The cells were harvested and processed for the flow cytometrical analysis to quantify the fluorescence intensity of the end-product of CM-DCF.

MITOCHONDRIAL MEMBRANE POTENTIAL ASSAY

The MMP of astrocytes was measured by flow cytometry with the lipophilic cationic probe, JC-1, as previously described [Yang et al., 2008]. Briefly, astrocytes (1×10^6 cells/60-mm dish) were treated with K_2CrO_4 for 6 and 12 h. The cells were then incubated with 10 μM of JC-1 for 30 min at 37°C. After the harvest, the cells were centrifuged, resuspended in a total volume of 1 ml, and analyzed by using FACS. Two excitation wavelengths, 527 nm (green) and 590 nm (red), were used to detect the JC-1 monomer form and the JC-1 aggregate form, respectively. The red fluorescence was predominantly detected in healthy cells with high MMP, while its level was decreased in damaged mitochondria. Alternatively, after astrocytes were exposed to 50 μM of K_2CrO_4 for 12 h, the cells were incubated with 10 μM of JC-1 for 30 min at 37°C and were fixed in 4% paraformaldehyde thereafter for 15 min. JC-1 staining in astrocytes was visualized under an epifluorescence microscope equipped with a cooling digital imaging system.

ELECTROPHORESIS MOTILITY SHIFT ASSAY

Nuclear proteins were extracted using the NE-PER kit according to the procedure of the manufacturer. The double-stranded DNA sequences specific for the binding of NF-κB and AP-1 were end-labeled with [^{32}P] using the T4 polynucleotide kinase at 37°C for 10 min. Nuclear protein extracts (20 μg) were incubated in the final volume of 20 μl binding buffer (10 mM Tris–HCl, pH 7.5, 250 mM NaCl, 5 mM $MgCl_2$, 2.5 mM EDTA, 2.5 mM dithiothreitol, and 5% glycerol) containing 1 μg poly-dIdC and 5 ng end-labeled oligomer at room temperature for 20 min. The reaction mixture was fractionated on a 6% polyacrylamide gel (2 h, 180 V). The gel was dried and exposed to film at −70°C for 1–2 h.

IMMUNOFLUORESCENCE

After treatment, the cells were fixed in PBS containing 4% paraformaldehyde for 10 min, followed by anti-GFAP (1:200), anti-AIF (1:80), or anti-EndoG (1:100) antibodies in PBS containing 5% horse serum at room temperature for 1 h. The cultures were incubated with biotinylated secondary antibodies (1:200) for 1 h, and subsequently FITC–avidin (1:200) was added to the cultures for 45 min. The

culture was subjected to nuclei counterstaining in PBS containing 1 μg/ml DAPI for 2 min. The results were observed under a fluorescence microscope equipped with a cooling CCD system.

STATISTICAL ANALYSIS

Data are expressed as mean ± SEM. Each experiment was repeated at least three times. Statistical significance of differences between the two groups of data (P-value < 0.05) was analyzed using two-tailed Student's t-test.

RESULTS

EXPOSURE TO Cr(VI) INDUCES ASTROCYTIC CELL APOPTOSIS

MTT cell viability and LDH assays were performed to examine the cell viability of Cr(VI)-primed neural cells. As shown in Figure 1A, Cr(VI) at concentrations of 0.01–10 μM did not affect astrocytic cell viability. Considerable reduction of astrocytic cell viability was observed at 6 h after treatment with Cr(VI) at 100 μM (8%), while substantial reduction by Cr(VI) at 50 μM (15%) was found at 12 h (Fig. 1A). Treatment with Cr(VI) at 30, 50, and 100 μM for 24 h caused 25%, 40%, and 60% reduction in astrocytic cell viability, respectively. These results indicate the dose- and time-dependent effect of Cr(VI) on the reduction of the astrocytic cell viability. We also observed that LDH release from the cultures was increased by Cr(VI) at 50 μM (10%) and 100 μM (18%) for 12 h (Fig. 1B). It was also noted that exposure of neurons to Cr(VI) at 30, 50, and 100 μM for 24 h reduced their cell viability by 50%, 70%, and 90% (Fig. 1C), while Cr(VI) at 50 and 100 μM can induce 40% and 60% reduction in the cell viability of microglia, CNS resident macrophages (Fig. 1D).

The morphological examination by using the immunofluorescence and DAPI nuclear staining indicated that astrocytes displayed the characteristic condensed nucleus after treatment with Cr(VI) at 30, 50, and 100 μM for 24 h (Fig. 2A–D). Moreover, the process retraction was observed in Cr(VI)-treated astrocytes. Furthermore, we found that DNA fragmentation was detected as early as 6 h in astrocytes treated with Cr(VI) at 50 and 100 μM (Fig. 2E). Since we observed substantial DNA laddering in astrocytes treated for 12 h with Cr(VI), a TUNEL assay for labeling DNA breaks with 3′-OH to quantify apoptotic cells by flow cytometry was performed after a 12-h treatment. As shown in Figure 2F, an increase in apoptotic cells was observed in the culture treated with Cr(VI) by a dose-related trend.

ROS GENERATION IN ASTROCYTES

Since DNA laddering in Cr(VI)-treated astrocytes was found as early as 6 h (Fig. 2E), ROS generation in astrocytes was examined

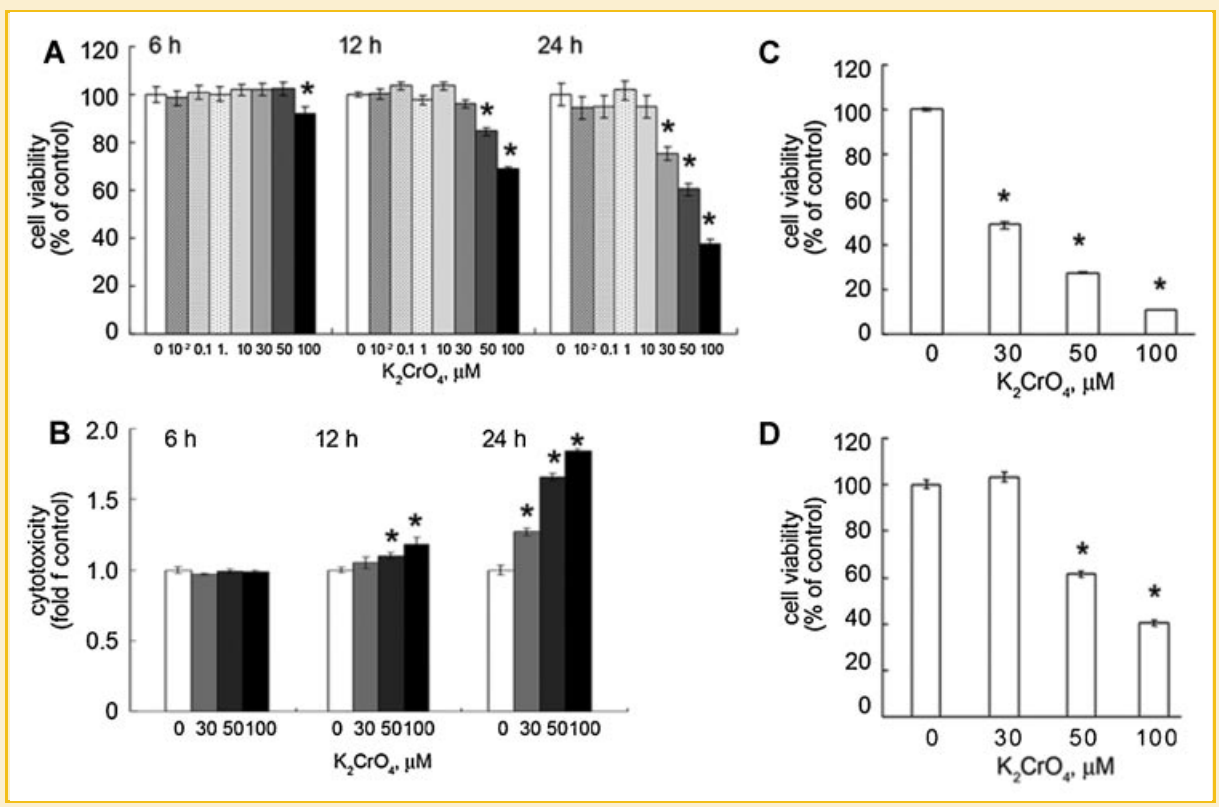

Fig. 1. Induction of cell death by Cr(VI) in glia and neurons. Astrocytes, neurons, and microglia were treated with different concentrations of K_2CrO_4 for the distinct time periods indicated as above. Cell viability was determined by MTT assay and revealed that exposure to Cr(VI) reduced the survival of astrocytes (A), neurons (C), and microglia (D). Astrocytic cell toxicity was examined by determining the relative levels of released LDH in the culture supernatant after treatment with different concentrations of K_2CrO_4 for the distinct time periods as indicated above (B). Data are mean ± SEM of at least three independent experiments. $^*P < 0.05$ versus control.

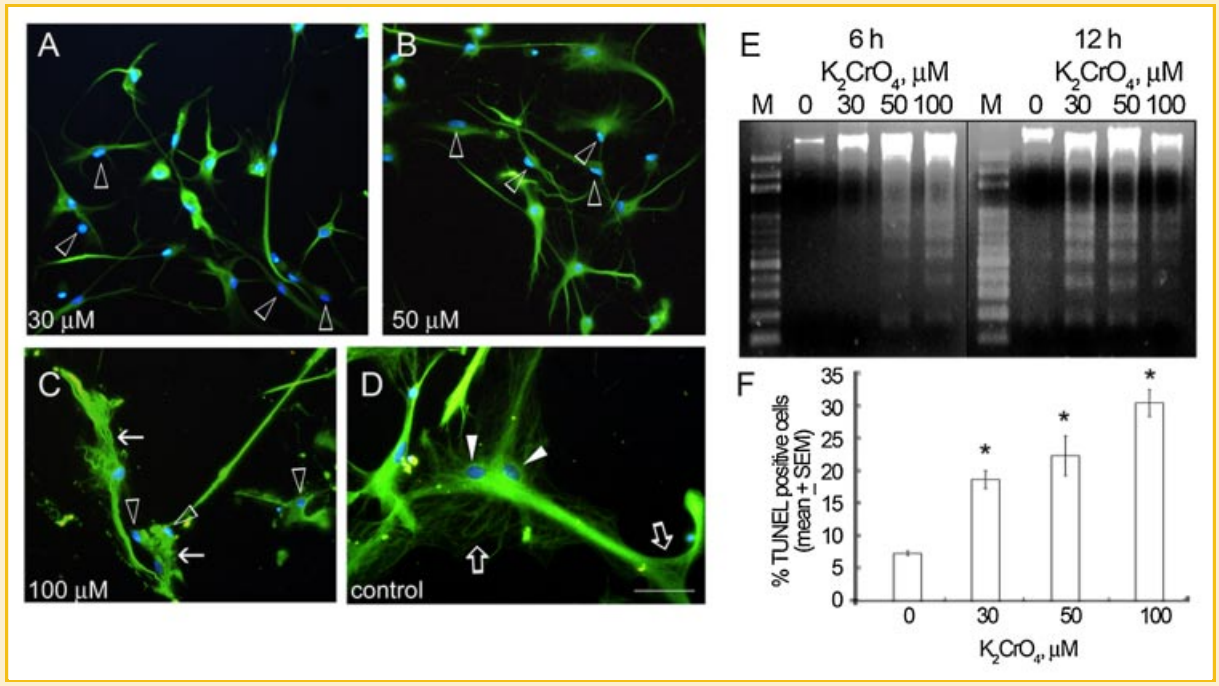

Fig. 2. Astrocytic apoptotic cell death induced by Cr(VI). A–D: Astrocytes were treated for 24 h with K_2CrO_4 at the concentrations as indicated above. Cell morphology was examined by GFAP immunostaining (green) combined with DAPI nuclear staining (blue), and revealed that shrinking condensed nuclei (open arrowheads) and disorganized filament cytoskeletons (arrows) were observed in Cr(VI)-treated astrocytes. Note that control astrocytes had the flat nuclei with diffusible DAPI staining (arrowheads) and well-organized cytoskeletal features (open arrows). Scale bar, 50 μm. E: Astrocytes were treated for 6 and 12 h with K_2CrO_4 at the concentrations as indicated above, and then subjected to genomic DNA extraction for DNA fragmentation analysis. M, 100 bp DNA ladder. F: Astrocytes were treated with K_2CrO_4 at 30, 50, and 100 μM for 12 h, and then processed for TUNEL assay using flow cytometry. Results shown are mean ± SEM of three independent experiments. $^*P < 0.05$ versus control.

at 6, 12, and 15 h after treatment with 50 and 100 μM of Cr(VI). As shown in Figure 3, Cr(VI) at 50 and 100 μM induced a significant increase in astrocytic ROS levels at 6, 12, and 15 h. In addition, ROS generation in Cr(VI)-primed astrocytes was increased time-dependently.

CASPASES-3 ACTIVATION IN Cr(VI)-PRIMED ASTROCYTES

Caspase-3 activation generally serves as an indicator of cell apoptosis because the active form of caspase-3 produced under the effect of several of upstream signaling pathways is needed to execute the final apoptosis [Riedl and Shi, 2004]. Since ROS levels

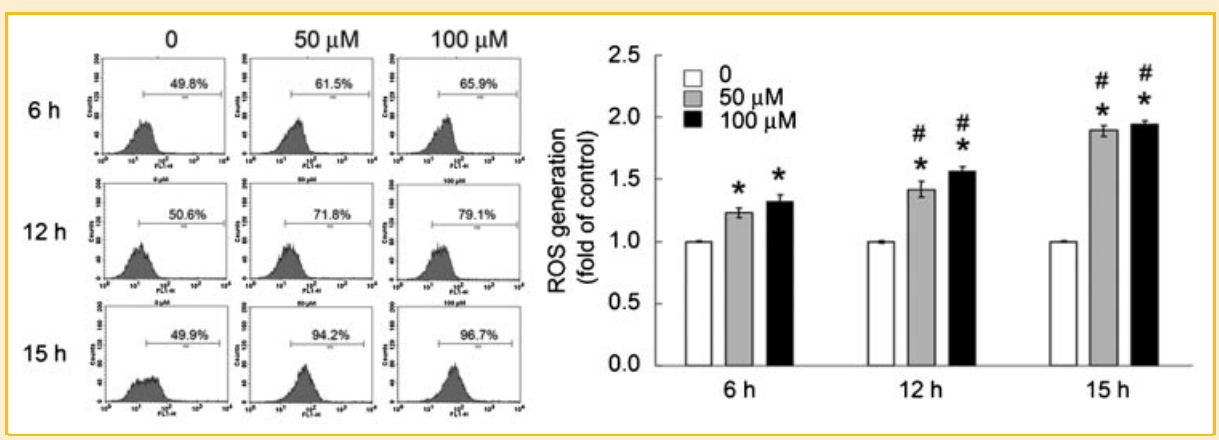

Fig. 3. Cr(VI)-induced generation of ROS in astrocytes. Astrocytes were treated with 50 and 100 μM of K_2CrO_4 for 6, 12, and 15 h, and then processed for flow cytometric analysis to measure ROS levels in astrocytes which preloaded with the ROS indicator CM-H_2DCFDA for 45 min. The pictures (left panel) shown are representative for three independent experiments performed. Data shown in the graph of the quantification (right panel) are mean ± SEM of three independent experiments. $^*P < 0.05$ versus the control culture at relative time point; $^\#P < 0.05$ compared with 6 h treatment.

were increased at 6 h after treatment with Cr(VI), the caspase-3 activity was examined at 6 and 12 h. The activity assay showed that a 50% increase in the caspase-3 activity was observed when astrocytes were exposed to Cr(VI) at 30, 50, and 100 μM for 12 h, but not for 6 h (Fig. 4A). Indeed, the cleaved form of the caspase-3 was also detected at 12 h in Cr(VI)-primed astrocytes (data not shown). A selective irreversible inhibitor of caspase-3, Z-DEVD-FMK, was used to examine whether caspase-3 was involved in astrocytic apoptosis. As shown in Figure 4B, pretreatment with Z-DEVD-FMK for 1 h effectively inhibited the caspase-3 activity in Cr(VI)-primed astrocytes at 12 h. However, the cell viability assay indicated that the cell death of Cr(VI)-primed astrocytes was not blocked by a 1-h pretreatment with Z-DEVD-FMK (Fig. 4C), demonstrating the involvement of the caspase-3 independent pathway in the regulation of astrocytic apoptosis.

AP-1 AND NF-κB DNA BINDING ACTIVITY

NF-κB and AP-1 are considered as the oxidant sensitive transcription factors since the two transcription factors play the central role in ROS-mediated gene expression [Dalton et al., 1999; Natarajan et al., 2002]. Thus, EMSA was performed to determine whether the binding of AP-1 and NF-κB to their specific elements was increased. As shown in Figure 5, the DNA binding activity of AP-1 was increased at 12 h in Cr(VI)-primed astrocytes. An increase in the DNA binding activity of NF-κB-p50/p50 was also observed at 2 h, and this decrease was seen at 12 h (Fig. 5). The involvement of ROS cascade-associated kinases (i.e., JNK, p38MAPK, and MEK/MAPK) in Cr(VI)-induced astrocytic cell death was also investigated. However, the inhibition of the AP-1 upstream molecules using SP600125 (JNK), SB203580 (p38MAPK), U0126 (MEK), and PD98059 (MAPK) did not blockade the effect of Cr(VI) on astrocytic

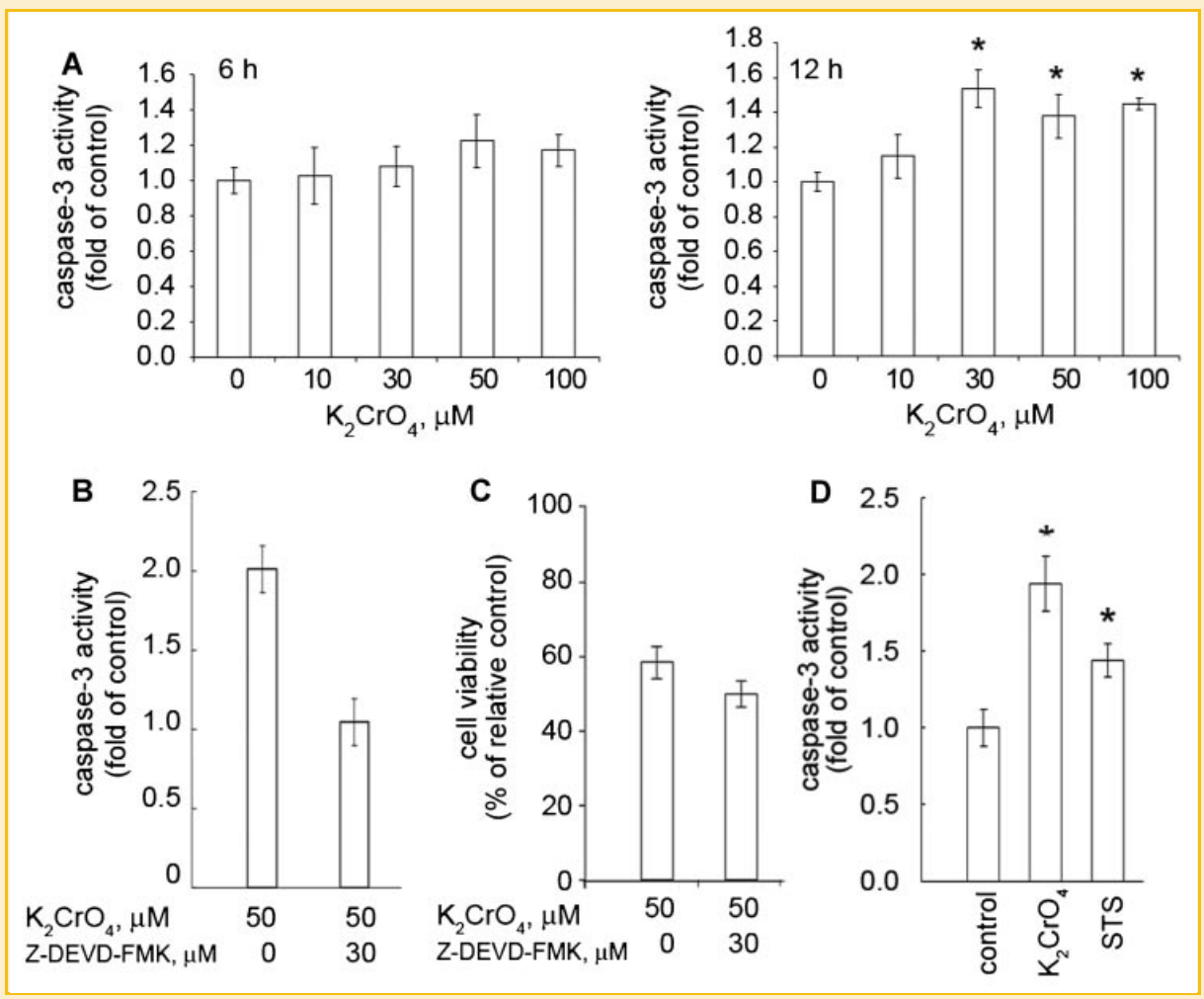

Fig. 4. Activation of caspase-3 in Cr(VI)-primed astrocytes. A: Astrocytes were treated for 6 and 12 h with K_2CrO_4 at the concentrations as indicated above, and then subjected to the caspase-3 activity assay. B: The effect of Z-DEVD-FMK on the inhibition of the caspase-3 activity was determined in astrocytes that were pretreated with 30 μM of Z-DEVD-FMK for 1 h, followed by 50 μM of K_2CrO_4 for 12 h. C: Astrocytes were pretreated with the caspase-3 inhibitor, Z-DEVD-FMK (30 μM) for 1 h, and then exposed to 50 μM of K_2CrO_4 for 24 h. The cell viability was determined by MTT assay. D: Astrocytes were treated for 12 h either with 50 μM of K_2CrO_4 or with 100 nM of staurosporine (STS), and then subjected to the analysis of caspase-3 activity. The STS-treated culture was used as a positive control for caspase-3 activity assay. Data are mean ± SEM of three independent experiments. $^*P < 0.05$.

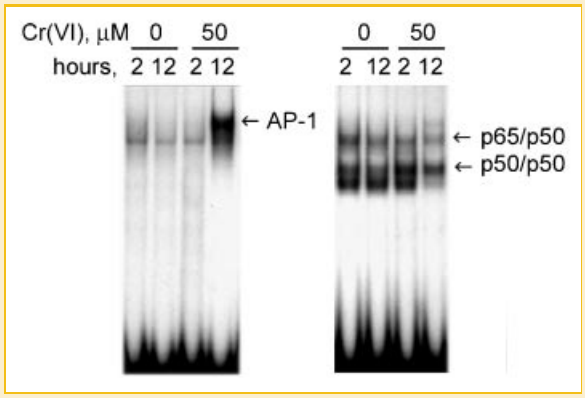

Fig. 5. AP-1- and NF-κB-DNA binding activity in Cr(VI)-primed astrocytes. Primary astrocytes treated with 50 μM of K_2CrO_4 for 2 and 12 h were analyzed by EMSA which was performed with labeled oligonucleotides containing the consensus sequences of AP-1 and NF-κB. The binding specificity was confirmed in the presence of unlabeled oligonucleotides (100-fold molar excess). DNA/p65/p50 and DNA/p50/p50 complexes were confirmed by examining the inhibition of the DNA binding when nuclear extracts were incubated with anti-p65 or anti-p50 antibodies in the presence of labeled probes (data not shown). The experiments were repeated twice with similar observations.

cell death (Supplementary Fig. 1). The results were consistent with the findings in a human non-small cell lung carcinoma CL3 cell line [Chuang et al., 2000].

REDUCTION OF MMP

We next tried to determine if mitochondrial membrane depolarization occurred in Cr(VI)-primed astrocytes by examining the reduction in the MMP. JC-1 staining indicated that well-organized punctate JC-1 aggregates were distributed in the control astrocytes (Fig. 6A, arrows). However, diffuse fluorescence of JC-1 aggregates was scattered in astrocytes after treatment with 50 μM of Cr(VI) for 12 h (Fig. 6A, arrowheads). In addition, the results from flow cytometry confirmed that exposure to Cr(VI) at 50 and 100 μM for 6 and 12 h caused 1.8–2.6-fold increases in MMP loss (Fig. 6B).

Based on the results shown above, ROS signaling is likely to play a critical role in the cell death of Cr(VI)-primed astrocytes. Thus, several antioxidants were used to examine whether these molecules can rescue astrocytes from Cr(VI)-induced oxidative toxicity. The antioxidants including SOD analog (MnTBAP), resveratrol, ellagic acid, α-tocopherol, and ascorbic acid had less effect on the protection of astrocytes from Cr(VI) insult (Supplementary Fig. 1).

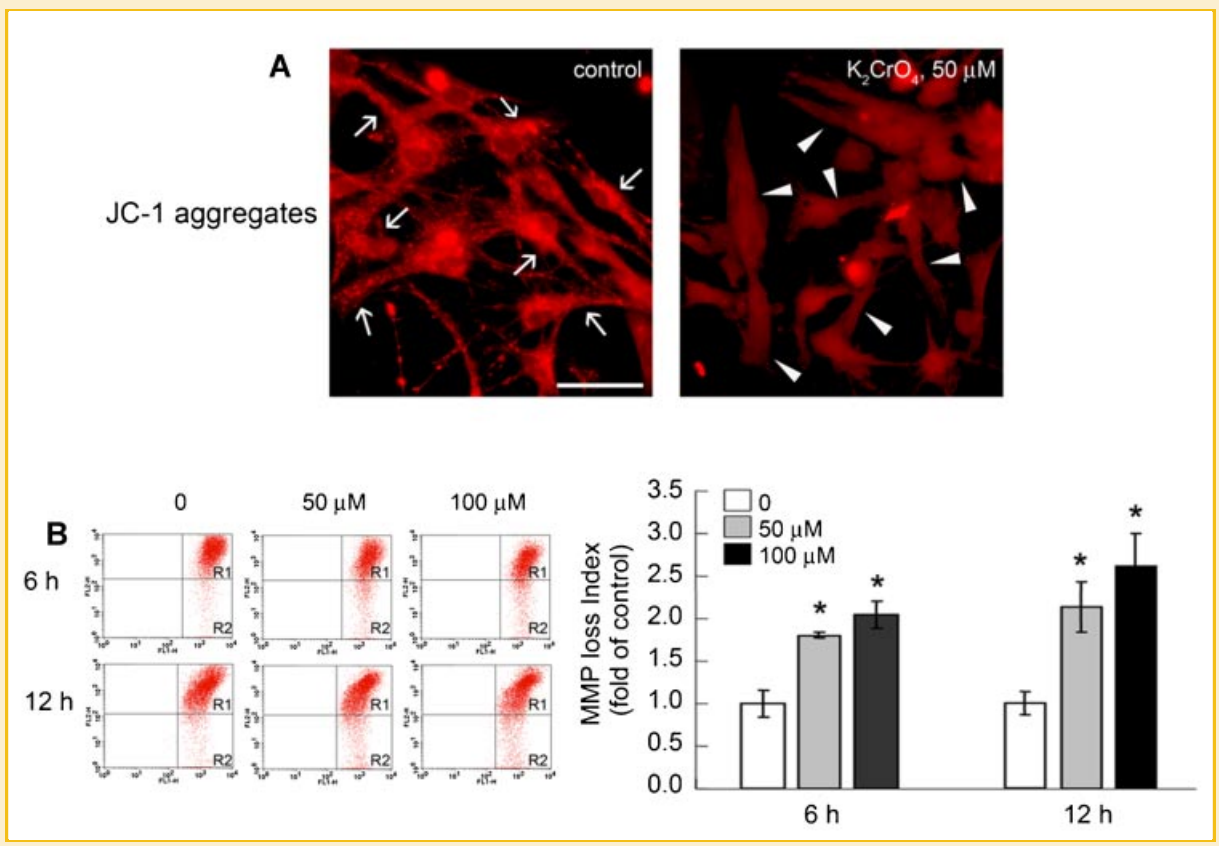

Fig. 6. Mitochondrial impairment in Cr(VI)-primed astrocytes. A: The strong punctate red fluorescence intensity (arrows) of aggregated cationic dye JC-1 complexes was detected in control astrocyte cultures, whereas a decrease observed in astrocytes treated with 50 μM of K_2CrO_4 (arrowheads) for 6 h. Scale bar, 50 μm. B: Astrocytic mitochondrial membrane potential (MMP) alteration was examined by flow cytometric analysis using JC-1 after treatment with 50 and 100 μM of K_2CrO_4 for 6 and 12 h. The pictures (left panel) shown are representative for three independent experiments performed. The quantification of the fluorescence intensity in the R2 region indicated that exposure to Cr(VI) for 6 and 12 h significantly caused MMP loss in astrocytes. Data are mean ± SEM of three independent experiments. $^*P < 0.05$.

Since NAC works as the potent ROS scavenger [Aruoma et al., 1989], we examined NAC effect on the ROS generation and cell viability of Cr(VI)-treated astrocytes. Pretreatment with NAC effectively reduced ROS production in Cr(VI)-treated astrocytes (Fig. 7A), and exerted significant protection against Cr(VI)-induced oxidative toxicity (Fig. 7B). Moreover, pre-exposure to NAC effectively restored MMP in Cr(VI)-primed astrocytes (Fig. 7C). It was also noted that the other antioxidants used for this study did not effectively reduce ROS generation in Cr(VI)-treated astrocytes. For example, MnTBAP, a cell permeable SOD mimetic, did not attenuate ROS generation in Cr(VI)-treated astrocytes (Fig. 7A), and failed to increase the cell viability of Cr(VI)-treated astrocytes (Supplementary Fig. 1).

NUCLEAR LOCALIZATION OF AIF AND EndoG IN ASTROCYTES

Nuclear AIF and EndoG are considered as the effectors involving in caspase independent cell apoptosis [Li et al., 2001; Cande et al., 2002; Cregan et al., 2002; Lorenzo and Susin, 2004]. Immunofluorescence showed that the clear punctate staining for AIF and the diffusible staining for EndoG were mostly found in the cytoplasma of the control astrocytes, but not in the nuclei (Fig. 8, arrows). Upon a 12-h exposure to Cr(VI), some of the cells showed AIF staining in their nuclei (Fig. 8A, arrowheads). In addition, the punctate staining for EndoG was observed in nuclei at 12 h in Cr(VI)-primed astrocytes (Fig. 8B, arrowheads). Western blotting also showed that the nuclear levels of AIF and EndoG were increased in Cr(VI)-treated astrocytes (Fig. 8E).

DISCUSSION

The present study showed that astrocytes after exposure to the potent oxidant metal, Cr(VI), displayed typical apoptotic appearances (i.e., nuclei condensation, cell shrinkage, and apoptotic

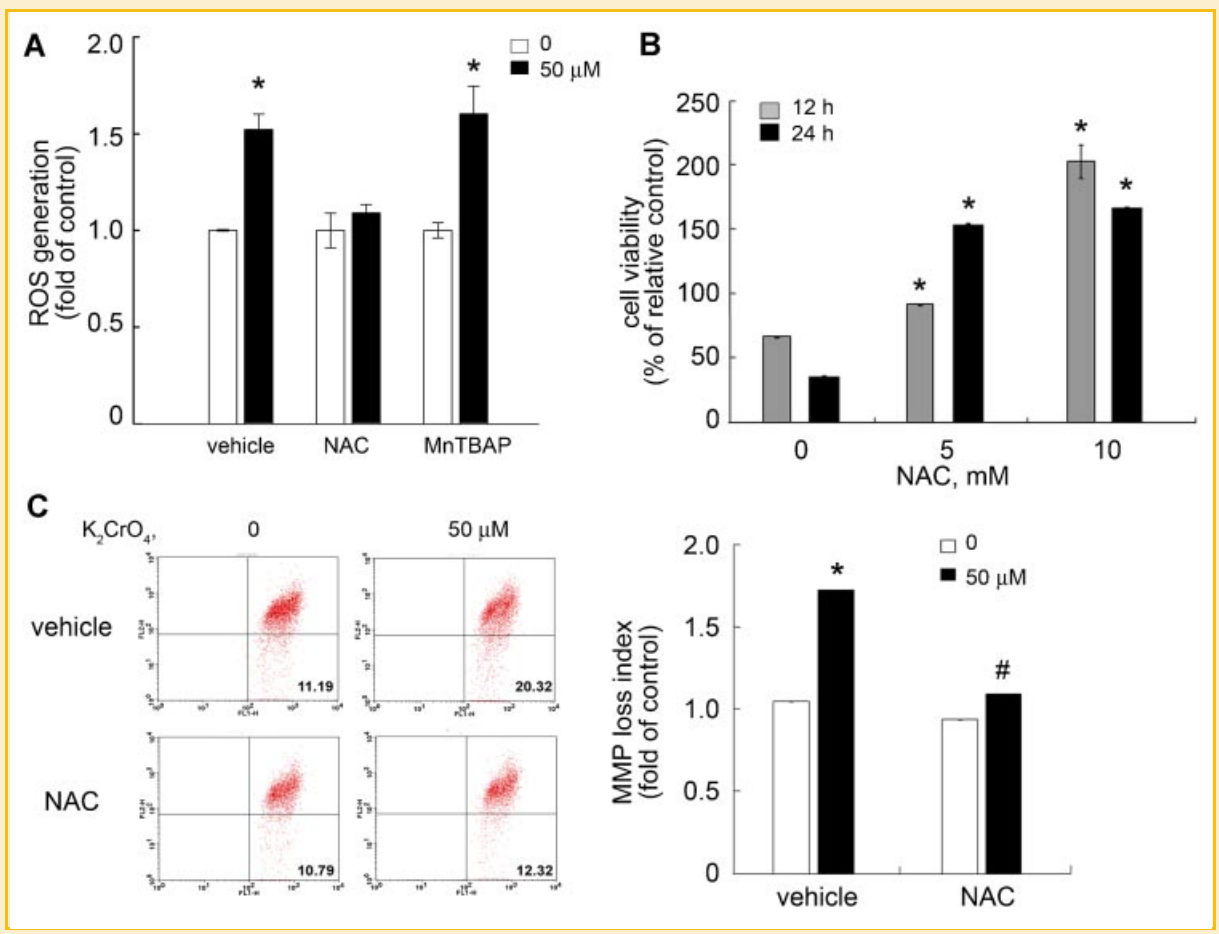

Fig. 7. Protective effect of *N*-acetylcysteine (NAC) on Cr(VI)-primed astrocytes. A: Astrocytes were pretreated with NAC (10 mM) and MnTBAP (50 μM), respectively. ROS levels in astrocytes were then examined at 6 h after treatment with Cr(VI). Data are mean ± SEM of three independent experiments. $^{*}P < 0.05$ versus control which was not treated with Cr(VI), NAC, or MnTBAP. B: MTT assay indicated that pretreatment with NAC (5 and 10 mM) for 1 h significantly increased astrocytic cell viability after exposure to 50 μM of K_2CrO_4 for 12 and 24 h. Data are mean ± SEM of at least three independent experiments. $^{*}P < 0.05$ versus control at each time point. C: After pretreatment of astrocytes with NAC (10 mM) for 1 h, the culture was exposed to 50 μM of K_2CrO_4 for 6 h. MMP loss in astrocytes was examined by flow cytometric analysis described as above. The pictures (left panel) shown are representative for three independent experiments performed. The quantification of the fluorescence intensity in the R2 region indicated that NAC effectively reduced the effect of Cr(VI) in astrocytic MMP loss. Data are mean ± SEM of three independent experiments. $^{*}P < 0.05$ versus to the control without any treatment. $^{\#}P < 0.05$ versus to the culture with Cr(VI) treatment only.

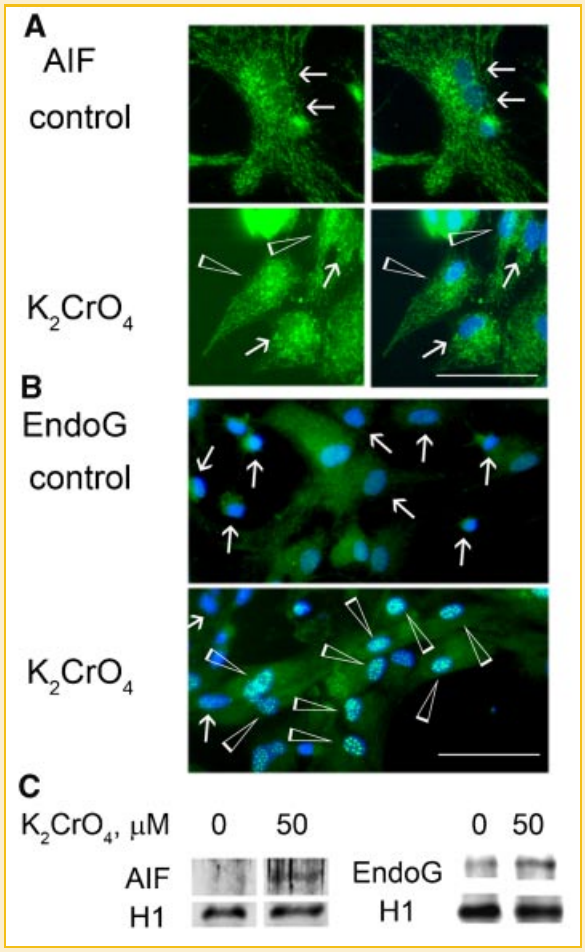

Fig. 8. Nuclear localization of AIF and EndoG in Cr(VI)-primed astrocytes. Astrocytes were treated with 50 μM of K_2CrO_4 for 12 h. AIF (A) and EndoG (B) was detected by immunofluorescence staining (green) combined with DAPI nuclear staining (blue). Arrows in (A) nuclear AIF (−); arrows in (B) punctate nuclear EndoG (−); arrowheads in (A) nuclear AIF (+); arrowheads in (B) punctate nuclear EndoG (+). Scale bar, 50 μm. C: Astrocytes were cultured in the presence or absence of 50 μM of K_2CrO_4 for 12 h, and then subjected to Western blotting for the analysis of the nuclear level of AIF and EndoG. The level of histone 1 (H1) protein was used as a loading control. Experiments were repeated twice with similar results.

bodies) along with DNA fragmentation, pointing to oxidative stress-induced apoptotic pathway in astrocytes. Although the caspase-3 activation occurred in Cr(VI)-primed astrocytes, the caspase-3 selective inhibitor, Z-DEVD-FMK, failed to increase astrocytic cell viability, indicating the uncoupling of the caspase-3 cascade to Cr(VI)-induced astrocytic apoptosis. Examination of the apoptotic effector proteins (AIF and EndoG), targeted by an ROS signaling pathway, appeared to show that nuclear translocation of AIF and EndoG could be caused by a loss of MMP in astrocytes. We also showed here that the antioxidant, NAC, inhibited ROS rise by Cr(VI), reduced the MMP loss, and efficiently prevent astrocytic cell death from Cr(VI) insult.

Exposure of neurons to Cr(VI) at concentrations above 30 μM significantly reduced their cell viability. In comparison with astrocytes, exposure to Cr(VI) resulted in the reduction of neuronal cell death to a greater extent. Astrocytes function as better scavengers for free radicals because antioxidants (such as, GSH) and antioxidative enzymes (i.e., SOD and GPx) are enriched in astrocytes [Kraig et al., 1995; Ransom et al., 2003; Li et al., 2008]. Therefore, astrocytes showed more resistance to Cr(VI) than neurons did (Fig. 1C). Evidence has also indicated that dysfunctional and reduced astrocytes can enhance neuronal degeneration by diminishing the secretion of trophic factors, pointing to the survival support for neurons from astrocytes [Takuma et al., 2004]. This provides explanations for more extensive cell death observed in primary neuronal cultures after Cr(VI)-induced oxidative insult than those seen in astrocytes.

Our finding of the significant morphological change in astrocytes observed 24 h after exposure to Cr(VI) is consistent with the recent finding in primary human skin fibroblasts [Rudolf et al., 2005]. C(VI) was shown to cause a pronounced change in cellular cytoskeleton since the straight F-actin fiber in human skin fibroblast became bent and intertwisted in shape after treatment with 15–45 μM of Cr(VI) [Rudolf et al., 2005]. Our study showed that higher concentrations (>30 μM) of Cr(VI) were required to cause the disruption of astrocyte-specific intermediate filament (GFAP) in rat astrocytes (Fig. 2). We also observed that cytoskeleton disruption in Cr(VI)-primed astrocytes occurred as early as 12 h post-treatment. The higher concentrations of Cr(VI) had to be used to cause the effective morphological change in rat astrocytes when compared to that used in human skin fibroblasts, indicating that rat astrocytes had a better antioxidant defense system against Cr(VI)-induced oxidative damage. Moreover, the Cr(VI) effect on astrocytic morphological alternation might represent an early indication of cell death. On the other hand, the findings from others have demonstrated that Cr(VI) induced the apoptosis of human lymphoma U937 cells by the Ca^{2+}-calpain and caspase-dependent signaling pathway [Hayashi et al., 2004]. However, no change in intracellular Ca^{2+} levels have been detected after astrocytes exposed to Cr(VI) (Supplementary Fig. 2). Moreover, treatment with the extracellular Ca^{2+} chelator (EGTA) or the intracellular Ca^{2+} chelator (BAPTA-AM) did not reduce the cell death of Cr(VI)-primed astrocytes (Supplementary Fig. 2). Nevertheless, it is likely that the same oxidant agent may trigger the distinct cellular signaling in the different cell types to induce cell apoptotic death. Perhaps distinct defense capabilities may equip the different cell types to cope with oxidative insult. In contrast to Cr(VI), redox-inactive metal ions (Cd^{2+}) has been reported to induce Ca^{2+} influx and cause oxidative injury in astrocytes [Yang et al., 2008].

Although our data showed that exposure to Cr(VI) resulted in the caspase-3 activation in astrocytes, the inhibition of caspase-3 activity failed to blockade the Cr(VI) cytotoxic effect on astrocytic cell death. Indeed, accumulated evidence has demonstrated that treatment with effective caspase inhibitors may not be sufficient to prevent cell death despite the induced activation of caspase-3 [Jaattela and Tschopp, 2003; Chipuk and Green, 2005; Kroemer and Martin, 2005]. This supports our observation that activated caspase-3 was not the major player in the induction of astrocytic death by Cr(VI). We have shown here that an increase in the caspase-3 activity was not observed at 6 h until a 12-h treatment with Cr(VI), while a significant loss of MMP in astrocytes occurred as early as 6 h

post-Cr(VI) exposure (Fig. 6). Since caspase-3 activation occurred after the mitochondrial membrane permeabilization, it is not considered a mechanism of cell death (Fig. 4). Thus, based on our findings, caspase-3 activation could be a cellular response to Cr(VI)-induced DNA damage. Nevertheless, further studies are needed to substantiate the role of activated caspase-3 in the response of astrocytes to Cr(VI).

Interruption of NF-κB activation in human bronchial epithelial cell line, BEAS-2B, by a kinase-mutated form of IκB kinase β (IKKβ) can promote Cr(VI)-induced cell death [Chen et al., 2002]. Interestingly, our results have shown that an increase in the DNA binding of NF-κB was observed at 2 h in Cr(VI)-primed astrocytes. Given the fact that quercitrin is found to be the potent inhibitor of IKKα and IKKβ, which in turn inhibits the NF-κB activation [Peet and Li, 1999], we used quercitrin to examine whether astrocytic cell death can be suppressed by quercitrin. However, our data have indicated that quercitrin showed no effect on Cr(VI)-induced astrocytic cell death (Supplementary Fig. 1). It is possible that NF-κB activation might be involved in the astrocytic defense mechanism against Cr(VI)-oxidative damage; however, NF-κB-induced protective action could not compensate for Cr(VI)-oxidative damage to astrocytes. These observations indicated that NF-κB activation might be an early event of Cr(VI)-induced oxidative stress.

We also observed that an increase in the DNA binding of AP-1 in astrocytes which occurred at the relatively late stage (12 h) after the Cr(VI) exposure. The activity of JNK and p38MAPK, which are known to induce AP-1 activation, has been reported to be increased by Cr(VI) via redox mechanisms, but irrelevant to Cr(VI) cytotoxicity of the non-small cell lung carcinoma cell line [Chuang et al., 2000]. Indeed, the inhibitors of JNK and p38MAPK are not able to reduce the Cr(VI) cytotoxic effect on astrocytes (Supplementary Fig. 1), indicating that AP-1 activation might occur as a cellular response to Cr(VI)-induced oxidative stress; however, it is not a factor that contributes to Cr(VI)-induced oxidative apoptosis in astrocytes.

Mitochondria damage that leads to an increase in intracellular levels of Ca^{2+} and ROS and to the release of effector proteins is thought to be involved in the caspase-independent cell death [Green and Kroemer, 2004]. The participation of Ca^{2+} in Cr(VI)-induced astrocytic death has been ruled out (Supplementary Fig. 2). Yet, our data shown here indicate that ROS levels in astrocytes were increased 6 h after the exposure to Cr(VI). In addition, a sustained and greater elevation of ROS level was observed in astrocytes at 12 and 15 h treatment with Cr(VI). Although several potential antioxidants (resveratrol, α-tocopherol, ellagic acid, α-tocopherol, β-carotene, and MnTBAP) failed to protect astrocytes against Cr(VI) insult, the potent antioxidant NAC not only effectively reduce ROS production and MMP loss in Cr(VI)-treated astrocytes, but also increase astrocytic cell viability in the presence of Cr(VI). It is also noted that antioxidants used in the study had no effect on the inhibition of ROS production in Cr(VI)-treated astrocytes. These findings reveal that exposure to Cr(VI) causes oxidative injury to astrocytes and its effect on astrocytic death can be blocked by NAC.

Two of the intracellular reductants, reduced GSH and glutathione reductase (GR), are required for the reduction of Cr(VI) to Cr(III) [Raghunathan et al., 2009]. GSH is oxidized into dimer GSSH along with Cr(VI) reduction and formed into Cr–GSH complexes. The reduction of GSSH into GSH is suppressed due to GR inhibition [Raghunathan et al., 2009], leading to the depletion of intracellular reduced GSH. However, we have shown here that exposure to Cr(VI) significantly raised the levels of intracellular GSH at 30 min, and the increase in GSH levels was continually detected in astrocytes treated with Cr(VI) at the later time points (Supplementary Fig. 3). Intracellular GSH levels could be maintained by rapid upregulation of glutamate cysteine ligase as cells are suffering from oxidative stress [Kitteringham et al., 2000; Raghunathan et al., 2009]. This could explain why sustained or increased levels of GSH in Cr(VI)-treated astrocytes were observed. It also indicates that pretreatment with NAC may not only act as an effective antioxidant, but also provide as a GSH precursor to protect astrocytes from Cr(VI) insult.

AIF is known to contribute to caspase-independent cell death, whereby its release from the mitochondria to the nucleus causes chromatin condensation and cell death [Joza et al., 2001; Cande et al., 2002; Ravagnan et al., 2002; Cheung et al., 2005]. Since the case of astrocytic cell death shown here is caspase-3-independent, we have suspected the contribution of AIF to the Cr(VI)-induced astrocytic cell death. This suggestion is supported by the findings that the increased nuclear levels of AIF were observed in Cr(VI)-primed astrocytes. In addition, we have found an increase in nuclear levels of another mitochondrial factor, EndoG, which also triggered caspase-independent cell death [Ravagnan et al., 2002]. Significant DNA fragmentation and AIF/EndoG nuclear expression were concurrently observed at the relatively late stages (12 and 24 h) of Cr(VI) exposure (Fig. 2 and Fig. 8). These observations pointed to the plausible involvement of AIF and EndoG in ROS/mitochondria-mediated mechanism for Cr(VI)-induced oxidative apoptosis of astrocytes.

Finally, our findings provide evidence indicating that the apoptosis of astrocytes can be induced by the cellular oxidative insult through mitochondria-mediated, but not caspase-3-dependent pathway, which may be involved in astrocytic apoptosis after CNS injury and lead to the progress of neurodegeneration.

ACKNOWLEDGMENTS

The authors thank Yu-Peng Liu and Mei-Chuan Chen for cell culture and technical assistance.

REFERENCES

Andersen JK. 2004. Oxidative stress in neurodegeneration: Cause or consequence? Nat Med 10:S18–S25.

Aruoma OI, Halliwell B, Hoey BM, Butler J. 1989. The antioxidant action of N-acetylcysteine: Its reaction with hydrogen peroxide, hydroxyl radical, superoxide, and hypochlorous acid. Free Radic Biol Med 6:593–597.

Bagchi D, Balmoori J, Bagchi M, Ye X, Williams CB, Stohs SJ. 2002. Comparative effects of TCDD, endrin, naphthalene and chromium (VI) on oxidative stress and tissue damage in the liver and brain tissues of mice. Toxicology 175:73–82.

Cande C, Cohen I, Daugas E, Ravagnan L, Larochette N, Zamzami N, Kroemer G. 2002. Apoptosis-inducing factor (AIF): A novel caspase-independent death effector released from mitochondria. Biochimie 84:215–222.

Chen Y, Swanson RA. 2003. Astrocytes and brain injury. J Cereb Blood Flow Metab 23:137–149.

Chen F, Vallyathan V, Castranova V, Shi X. 2001. Cell apoptosis induced by carcinogenic metals. Mol Cell Biochem 222:183–188.

Chen F, Bower J, Leonard SS, Ding M, Lu Y, Rojanasakul Y, Kung HF, Vallyathan V, Castranova V, Shi X. 2002. Protective roles of NF-kappa B for chromium(VI)-induced cytotoxicity is revealed by expression of Ikappa B kinase-beta mutant. J Biol Chem 277:3342–3349.

Cheung EC, Melanson-Drapeau L, Cregan SP, Vanderluit JL, Ferguson KL, McIntosh WC, Park DS, Bennett SA, Slack RS. 2005. Apoptosis-inducing factor is a key factor in neuronal cell death propagated by BAX-dependent and BAX-independent mechanisms. J Neurosci 25:1324–1334.

Chipuk JE, Green DR. 2005. Do inducers of apoptosis trigger caspase-independent cell death? Nat Rev Mol Cell Biol 6:268–275.

Chuang SM, Liou GY, Yang JL. 2000. Activation of JNK, p38 and ERK mitogen-activated protein kinases by chromium(VI) is mediated through oxidative stress but does not affect cytotoxicity. Carcinogenesis 21:1491–1500.

Costa M, Klein CB. 2006. Toxicity and carcinogenicity of chromium compounds in humans. Crit Rev Toxicol 36:155–163.

Cregan SP, Fortin A, MacLaurin JG, Callaghan SM, Cecconi F, Yu SW, Dawson TM, Dawson VL, Park DS, Kroemer G, Slack RS. 2002. Apoptosis-inducing factor is involved in the regulation of caspase-independent neuronal cell death. J Cell Biol 158:507–517.

Dalton TP, Shertzer HG, Puga A. 1999. Regulation of gene expression by reactive oxygen. Annu Rev Pharmacol Toxicol 39:67–101.

Ding M, Shi X. 2002. Molecular mechanisms of Cr(VI)-induced carcinogenesis. Mol Cell Biochem 234–235:293–300.

Green DR, Kroemer G. 2004. The pathophysiology of mitochondrial cell death. Science 305:626–629.

Harris GK, Shi X. 2003. Signaling by carcinogenic metals and metal-induced reactive oxygen species. Mutat Res 533:183–200.

2004. Hayashi Y, Kondo T, Zhao QL, Ogawa R, Cui ZG, Feril LB, Jr., Teranishi H, Kasuya M, 2004. Signal transduction of p53-independent apoptotic pathway induced by hexavalent chromium in U937 cells. Toxicol Appl Pharmacol 197:96–106.

Jaattela M, Tschopp J. 2003. Caspase-independent cell death in T lymphocytes. Nat Immunol 4:416–423.

Joza N, Susin SA, Daugas E, Stanford WL, Cho SK, Li CY, Sasaki T, Elia AJ, Cheng HY, Ravagnan L, Ferri KF, Zamzami N, Wakeham A, Hakem R, Yoshida H, Kong YY, Mak TW, Zuniga-Pflucker JC, Kroemer G, Penninger JM. 2001. Essential role of the mitochondrial apoptosis-inducing factor in programmed cell death. Nature 410:549–554.

Kasprzak KS. 2002. Oxidative DNA and protein damage in metal-induced toxicity and carcinogenesis. Free Radic Biol Med 32:958–967.

Kitteringham NR, Powell H, Clement YN, Dodd CC, Tettey JN, Pirmohamed M, Smith DA, McLellan LI, Kevin Park B. 2000. Hepatocellular response to chemical stress in CD-1 mice: Induction of early genes and gamma-glutamylcysteine synthetase. Hepatology 32:321–333.

Koehler RC, Gebremedhin D, Harder DR. 2006. Role of astrocytes in cerebrovascular regulation. J Appl Physiol 100:307–317.

Kraig RLC, Caggiano A. 1995. Glial response to brain ischemia. In: Kettenmann HRB, editor. Neuroglia. New York: Oxford University Press. p. 964–976.

Kroemer G, Martin SJ. 2005. Caspase-independent cell death. Nat Med 11: 725–730.

Li LY, Luo X, Wang X. 2001. Endonuclease G is an apoptotic DNase when released from mitochondria. Nature 412:95–99.

Li G, Cui G, Tzeng NS, Wei SJ, Wang T, Block ML, Hong JS. 2005. Femtomolar concentrations of dextromethorphan protect mesencephalic dopaminergic neurons from inflammatory damage. FASEB J 19:489–496.

Li L, Lundkvist A, Andersson D, Wilhelmsson U, Nagai N, Pardo AC, Nodin C, Stahlberg A, Aprico K, Larsson K, Yabe T, Moons L, Fotheringham A, Davies I, Carmeliet P, Schwartz JP, Pekna M, Kubista M, Blomstrand F, Maragakis N, Nilsson M, Pekny M. 2008. Protective role of reactive astrocytes in brain ischemia. J Cereb Blood Flow Metab 28:468–481.

Lorenzo HK, Susin SA. 2004. Mitochondrial effectors in caspase-independent cell death. FEBS Lett 557:14–20.

Love S. 1999. Oxidative stress in brain ischemia. Brain Pathol 9:119–131.

McCarthy KD, de Vellis J. 1980. Preparation of separate astroglial and oligodendroglial cell cultures from rat cerebral tissue. J Cell Biol 85:890–902.

Natarajan R, Fisher BJ, Jones DG, Ghosh S, Fowler AA III. 2002. Reoxygenating microvascular endothelium exhibits temporal dissociation of NF-kappaB and AP-1 activation. Free Radic Biol Med 32:1033–1045.

O'Brien TJ, Ceryak S, Patierno SR. 2003. Complexities of chromium carcinogenesis: Role of cellular response, repair and recovery mechanisms. Mutat Res 533:3–36.

Peet GW, Li J. 1999. IkappaB kinases alpha and beta show a random sequential kinetic mechanism and are inhibited by staurosporine and quercetin. J Biol Chem 274:32655–32661.

Raghunathan VK, Tettey JN, Ellis EM, Grant MH. 2009. Comparative chronic in vitro toxicity of hexavalent chromium to osteoblasts and monocytes. J Biomed Mater Res A 88:543–550.

Ransom B, Behar T, Nedergaard M. 2003. New roles for astrocytes (stars at last). Trends Neurosci 26:520–522.

Ravagnan L, Roumier T, Kroemer G. 2002. Mitochondria, the killer organelles and their weapons. J Cell Physiol 192:131–137.

Riedl SJ, Shi Y. 2004. Molecular mechanisms of caspase regulation during apoptosis. Nat Rev Mol Cell Biol 5:897–907.

Rudolf E, Cervinka M, Cerman J, Schroterova L. 2005. Hexavalent chromium disrupts the actin cytoskeleton and induces mitochondria-dependent apoptosis in human dermal fibroblasts. Toxicol In Vitro 19:713–723.

Shi X, Dalal NS. 1994. Generation of hydroxyl radical by chromate in biologically relevant systems: Role of Cr(V) complexes versus tetraperoxochromate(V). Environ Health Perspect 102:231–236.

Sugiyama M, Patierno SR, Cantoni O, Costa M. 1986. Characterization of DNA lesions induced by CaCrO4 in synchronous and asynchronous cultured mammalian cells. Mol Pharmacol 29:606–613.

Takuma K, Baba A, Matsuda T. 2004. Astrocyte apoptosis: Implications for neuroprotection. Prog Neurobiol 72:111–127.

Tiffany-Castiglioni E, Sierra EM, Wu JN, Rowles TK. 1989. Lead toxicity in neuroglia. Neurotoxicology 10:417–443.

Voutsinos-Porche B, Bonvento G, Tanaka K, Steiner P, Welker E, Chatton JY, Magistretti PJ, Pellerin L. 2003. Glial glutamate transporters mediate a functional metabolic crosstalk between neurons and astrocytes in the mouse developing cortex. Neuron 37:275–286.

Yang CS, Tzou BC, Liu YP, Tsai MJ, Shyue SK, Tzeng SF. 2008. Inhibition of cadmium-induced oxidative injury in rat primary astrocytes by the addition of antioxidants and the reduction of intracellular calcium. J Cell Biochem 103:825–834.